Best relative sampling frequency of time-frequency-domain interferometry

Ming Wang#, Qun Hao, Qiudong Zhu, Yao Hu

Opto-Electronic College, Beijing Institute of Technology, Beijing 100081, China
Corresponding Author / E-mail: wang0425@gmail.com, TEL: +86-10-81619703

KEYWORDS : Phase-shifting interferometry, Anti-vibration, Time-frequency-domain method, Best relative sampling frequency

A time-frequency-domain (TFD) phase-shifting interferometry immune to environmental noises is proposed. A large number of phase-shifing interferograms are captured. The phase-shifting steps are not taken as a parameter, but the timing series of intensity array from each pixel. A series of distorted phase is obtained through broadband filtering and inverse Fourier transform to the spectrum of a series of intensity from a particular pixel. For a large enough number of interferograms, a linear statistics of the distorted phase array efficiently reduces random noises into zero. Other nonrandom noises are astringed into a nonzero value, which is independent to index of pixels and therefore does not influence shape of the whole wave front, only introducing a piston phase shift. Simulations of anti-vibration ability are carried out, reflecting the importance of optimizing relative sampling frequency which is the ratio between sampling frequency and phase-shifting frequency. The best relative sampling frequency is determined through theoretical analysis and mathematical simulations, which essentially explains advantages of TFD phase-shifting interferometry.

Manuscript received: January XX, 2011 / Accepted: January XX, 2011

NOMENCLATURE

OPD=optical path distance
TSD=time-spatial-domain
TFD = time-frequency-domain
AFP = amplitude-frequency product

1. Introduction

Phase-shifting interferometry has been the preferred technique in surface testing of optical elements for more than 30 years, especially in testing large-aperture elements or in long OPD systems. Early interferometry accomplished phase shift through movement of piezoelectric transducer [1] and obtained original phase by timing algorithms such as 4-step algorithm. In field testing, it was extremely limited by its high sensitivity to vibrations. Leslie L. Deck proposed a mathematical model of testing errors in presence of vibrations [2] to correct the errors for 7-step and 13-step algorithms. However, "it will be definitely unavailable when the vibration amplitude is beyond 60nm" [3]. Dynamic interferometry without moving elements has been developed for years. Instantaneous phase-shifting interferometry [4] suppressed time-varying noises by freezing interferograms at a moment, but is complicated in fabrication, especially for Fizeau interferometer. A new type of dynamic measurement system comprised of a micropolarizer array was invented by James E. Millerd[5] and then improved[6]. The unique configuration was easily adopted to both Twyman-Green and Fizeau type interferometers, but suffered from the reduction of spatial resolution and the high cost of pixelated phase-mask. A wavelength tuning phase-shifting interferometry[7] is developed for mini type Fizeau interferometer without moving any elements or reducing spatial resolution. Mechanic stability is easy to address, which guarantees higher immunity to vibrations of a large aperture system. However, for time domain algorithms, how much wavelength should be tuned for particular phase-shifting steps is determined by measured OPD. A Fourier transform algorithm applied in wavelength tuning system is proposed by Leslie Deck [8]. The measured original phase is obtained from the peak dot of the foundational frequency in spectrum of intensity array from a particular pixel. However, the required peak in spectrum can be easily overwhelmed in presence of vibrations, which leads failure in digging the foundational frequency. Furthermore, necessity of correcting nonlinearity of phase-shifting rate complicates the system much further.

In a word, the methods above suffer from either complexity of system or sensitivity to vibrations. A time-spatial-domain (TSD) random phase-shifting interferometry immune to environmental noises was recently proposed and applied to a minitype Fizeau interferometer [9]. Noises were averaged to a value which was the

same for different pixels and therefore did not influent the shape of the wave front. However, in order to implement ergodicity, a sampling frequency about 50 times of active phase-shifting rate was always required [10]. It extremely restrained the active phase-shifting rate under a fixed CCD device and thus limited anti-vibration ability of the system. In this paper, a TFD method based on the random phase-shifting algorithm is proposed. Neither accurate phase shift step nor linear phase shifter is required. Even the exact position of foundational frequency in spectrum of intensity array is not needed. Original phase is obtained through a frequency domain broadband filter and a time domain linear statistics. The measuring accuracy of TFD method is greatly influenced by the relative sampling frequency, which is defined as the ratio between sampling frequency and phase-shifting frequency. The best relative sampling frequency in TFD method is much lower than 50, which allows much higher phase-shifting frequency under the same hard device condition, and enhances the anti-vibration ability of TFD interferometry system over TSD method.

2. Principle of TFD phase-shifting interferometry

During continuous phase-shifting, intensity series from a particular pixel (x, y) in presence of environmental noises is written as:

$$I(x,y,t) = I_0\left\{1+V\cos\left[2\pi f_0 t+\varphi(x,y)+\delta(t)+\delta_r(x,y,t)\right]\right\} \quad (1)$$

where I_0 presents average intensity, V the contrast, f_0 the linear component of phase-shifting rate (moving f_0 interference fringes per second). $\varphi(x, y)$ is the phase to be measured in pixel (x, y), $\varphi_r(x, y, t)$ equivalent random distortion caused by air-turbulence and CCD noise. $\delta(t)$ is phase distortion introduced by vibrations and nonlinear phase-shifting rate, and is expressed as $\delta(t)= \delta_v(t)+ \delta_{nl}(t)$, with

$$\delta_v(t) = \sum 2\pi c_i \cos\left(2\pi f_{vi}t+\gamma_i\right),$$

$$\delta_{nl}(t) = 2\pi\left(a_1 f_1 t + a_2 f_2 t^2 + \cdots\right)t,$$

where c_i is the amplitude of the ith vibration component, f_{vi} the frequency, γ_i the starting phase; $a_i f_i t_i$ the ith order nonlinearity of phase-shifting rate.

Eq. (1) is transformed into frequency domain and the spectrum is demonstrated in Fig. 1, with a phase-shifting frequency of 20 Hz.

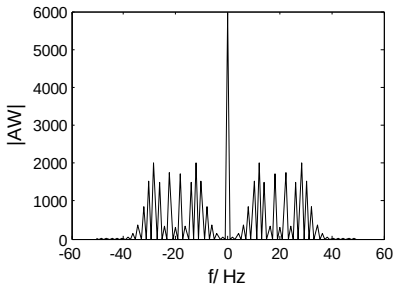

Fig. 1 Spectrum of intensity series from a particular pixel

The peak of foundational frequency in Fig. 1 is almost overwhelmed, and then the Fourier transform method in Ref. [8] is obviously unavailable now. Because of the high level of the zero frequency, DC term of Eq. (1) is firstly removed before Fourier transform in order to avoid overlap between zero frequency and broadened foundational frequency. Then the signal of interest in Eq. (1) is rewritten as:

$$s(x,y,t_n) = \frac{I_0 V}{2}\left\{\exp\left[i\left(2\pi f_0 t_n+\varphi(x,y)+\delta(t_n)+\delta_{rn}(x,y)\right)\right]\right. \\ \left.+\exp\left[-i\left(2\pi f_0 t_n+\varphi(x,y)+\delta(t_n)+\delta_{rn}(x,y)\right)\right]\right\} \quad (2)$$

Spectrum of Eq. (2) is calculated with Fourier transform, producing:

$$S(x,y,f_n) = \frac{I_0 V}{2}\left\{A(x,y,f_n)+A^*(x,y,f_n)\right\} \quad (3)$$

With $A(x, y, f_n)$ represents the Fourier transform of the positive term of Eq. (2), and A^* is the complex conjugate of A. Eq. (3) is demonstrated in Fig. 2, where the foundational frequency of 20 is emphasized with a heavy dot.

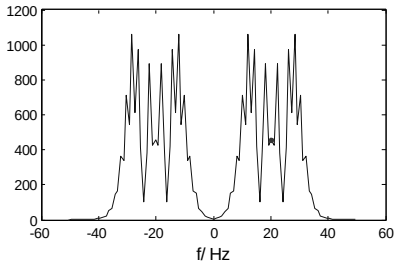

Fig. 2. Spectrum of intensity series of interest

A wide enough filter window covering the whole positive half of spectrum in Fig. 2 is applied to filter Eq. (3) and $A(x, y, f_n)$ is entirely reserved, differing from normal band-passing filtering in digital signal processing. All the phase information in $A(x, y, f_n)$, including the measured phase and the distorted phase introduced by noises, are extracted by the inverse Fourier transform of $A(x, y, f_n)$ produces:

$$\xi(x,y,t_n) = \frac{I_0 V}{2}\exp\left[i\left(2\pi f_0 t_n+\varphi(x,y)+\delta(t_n)+\delta_{rn}(x,y)\right)\right] \quad (4)$$

After a logarithm to Eq. (4), a series of distorted phase is obtained from the imaginary part of the result, expressing as:

$$\Phi(x, y, t_n) = \mathcal{W}\{2\pi f_0 t_n)+\varphi(x, y)+\delta(t_n)+\delta_{rn}(x, y) \quad (5)$$

where $\mathcal{W}$ is a temporal unwrapping operator. The unwrapped series of distorted phase is shown in Fig. 3.

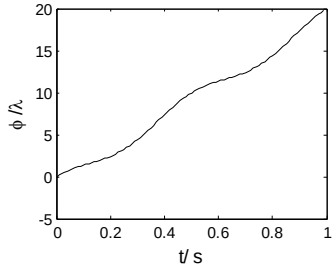

Fig. 3. Unwrapped phase array

In Fig. 3, the term of $2\pi f_0 t_n$ produces a large tilt and introduces the necessity of temporal $\mathcal{W}$ operation. With the purpose of efficiency, selected $A(x, y, f_n)$ from Eq. (3) is shifted by $-f_0$ before inverse Fourier transform operation, removing the tilt in Fig. 3. Then Eq. (5) is rewritten as:

$$\Phi(x,y,t_n) = \varphi(x,y)+\delta(t_n)+\delta_{rn}(x,y) \quad (6)$$

With N frames of phase-shifting interferograms, a linear statistics of Eq. (6) results in:

$$\bar{\Phi}(x,y,t_n) = \frac{1}{N}\left[N\varphi(x,y)+\sum_N \delta(t_n)+\sum_{n=1}^{N}\delta_{rn}(x,y)\right] \\ = \varphi(x,y)+\Delta\Phi+\frac{1}{N}\sum_{n=1}^{N}\delta_{rn}(x,y) \quad (7)$$

There are three terms in Eq. (7). $\varphi(x, y)$ is the target of the measurement and should be dealt with unwrapping operator, $\Delta\Phi$ is the digital mean of distorted phase introduced by nonrandom noise $\delta(t_n)$, and the third term is the mathematical average of random

noises over the phase-shifting acquisition. With a large number of interferograms over a long enough time, random phase distortion caused by the term $\delta_{rn}(x,y)$ are averaged into zero, which efficiently reduces the influence of random noise. The term $\Delta\Phi$ is independent to pixel index (*x*,*y*), thus it does not influence the phase distribution of whole wave front. Therefore, the unwrapped $\bar{\Phi}(x,y,0)$ has the same shape with the original wave front, only differs from a piston phase shift of $\Delta\Phi$ over the whole aperture.

3. Simulations for anti-vibration ability

For different original phase $\varphi(x,y)$ in Eq. (1) in presence of a single vibration with a frequency of 2Hz and an amplitude of 0.85λ, the series of calculating errors between $\bar{\Phi}(x,y,0)$ and $\varphi(x,y)$ are shown in Fig. 4. Although every single result deviates the true value by about 0.025λ, the PV value of error series is smaller than 0.0002λ, which verifies accuracy of surface measurement. Under the same condition, the accuracy of the TSD random phase-shifting interferometry in [9] is larger than 1λ, which presents the advantage of TFD method over the TSD method.

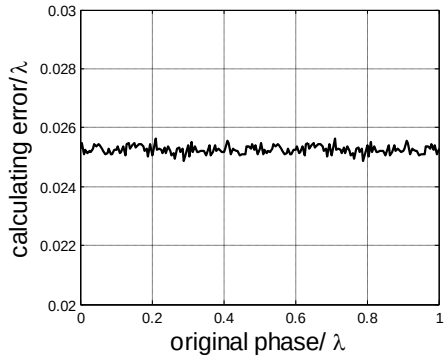

Fig. 4. Calculating errors for different original phase.

There are several factors influencing the measuring accuracy of TFD method, such as numbers of frames, sampling frequency and phase-shifting frequency.

For different numbers of captured interferograms and aiming at an accuracy of PV=λ/100, the maximum AFP of vibration are shown in Fig. 5.

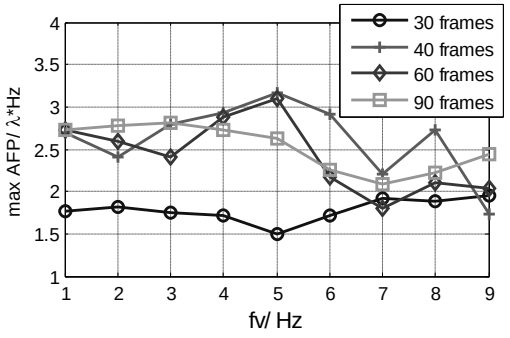

Fig. 5. Maximum AFP with different numbers of frame

When the numbers of frames are larger than 40, the maximum AFP stays at the same level, with a minor decrease with vibration frequency increasing. Therefore, it is infeasible to enhance the anti-vibration ability merely through increasing the numbers of interferograms.

With a fixed phase-shifting frequency of 25 Hz, a pure vibration with a frequency of 2Hz and amplitude of 0.85λ is introduced into the phase-shifting interferometry acquisition, and 100 frames of interferograms are captured. The PV values of wave front test accuracy under different sampling frequencies are shown in Fig. 6.

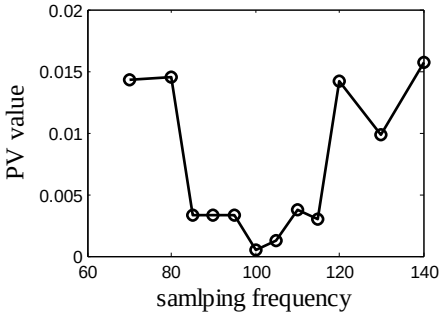

Fig. 6. PV value with different sampling frequency

When the sampling frequency varies with a fixed phase-shifting frequency, the PV values of measuring accuracy are quite different. In process of discrete Fourier transform, the relative sampling frequency which is the ratio between sampling frequency and phase-shifting frequency is the most important parameter, but not the sampling frequency or phase-shifting frequency individually. Then the best relative sampling frequency is required to maximize the anti-vibration ability of TFD interferometry.

4. Best relative sampling frequency of TFD method

It is assumed that there is a pure vibration tone during a TFD acquisition, and Eq. (1) is rewritten as:

$$I(x,y,t)=I_0\left\{1+V\cos\left[2\pi f_0 t+\varphi(x,y)+r\cos(2\pi f_v t+\alpha)\right]\right\} \tag{8}$$

with *r* represents the amplitude of vibration, f_v the frequency, and α the starting phase.

Eq. (2) is then rewritten as:

$$\begin{aligned} s(x,y,t_n)=\frac{I_0V}{2}\{&\exp\left[i(\varphi(x,y))\right]\exp(i\beta(t_n)) \\ &+\exp\left[-i(\varphi(x,y))\right]\exp(-i\beta(t_n))\} \end{aligned} \tag{9}$$

with $\beta(t_n)=2\pi f_0 t_n+r\cos(2\pi f_v t_n+\alpha)$ represents the real phase shifting during the acquisition. Utilizing the Jacobi-Anger expansion, Bessel functions properties and integrating over a detector integration period τ, Eq. (8) becomes:

$$\begin{aligned} s(x,y,t_n)=&\frac{I_oV}{2}J_0(r)\sin c(\pi f_0\tau)\exp(i\varphi(x,y)+2\pi i f_0 t_n) \\ &+\frac{I_oV}{2}J_0(r)\sin c(\pi f_0\tau)\exp(-i\varphi(x,y)-2\pi i f_0 t_n) \\ &+\frac{I_oV}{2}\sum_{k=1}^{\infty}i^kA_1(k)\exp(i2\pi t_n(f_o+kf_v)) \\ &+\frac{I_oV}{2}\sum_{k=1}^{\infty}i^kA_2(k)\exp(i2\pi t_n(f_o-kf_v)) \\ &+\frac{I_oV}{2}\sum_{k=1}^{\infty}(-i)^kA_3(k)\exp(i2\pi t_n(-f_o+kf_v)) \\ &+\frac{I_oV}{2}\sum_{k=1}^{\infty}(-i)^kA_4(k)\exp(i2\pi t_n(-f_o-kf_v)) \end{aligned} \tag{10}$$

with $A_1(k)=J_k(r)\sin c(\pi\tau(f_0+kf_v))\exp(i\varphi(x,y)+ik\alpha)$,
$A_2(k)=J_k(r)\sin c(\pi\tau(f_0-kf_v))\exp(i\varphi(x,y)-ik\alpha)$,
$A_3(k)=J_k(r)\sin c(\pi\tau(-f_0+kf_v))\exp(-i\varphi(x,y)+ik\alpha)$,
$A_4(k)=J_k(r)\sin c(\pi\tau(-f_0-kf_v))\exp(-i\varphi(x,y)-ik\alpha)$.

The spectrum is calculated with the Fourier transformer, producing:

$$\begin{aligned} S(x,y,f_n) &= \frac{I_o V}{2} J_0(r)\sin c(\pi f_0 \tau)\exp\left(i\varphi(x,y)\right)\delta(f_n - f_0) \\ &+ \frac{I_o V}{2} J_0(r)\sin c(\pi f_0 \tau)\exp\left(-i\varphi(x,y)\right)\delta(f_n + f_0) \\ &+ \frac{I_o V}{2}\sum_{k=1}^{\infty} i^k A_1(k)\delta(f_n - f_o - kf) \\ &+ \frac{I_o V}{2}\sum_{k=1}^{\infty} i^k A_2(k)\delta(f_n - f_o + kf) \\ &+ \frac{I_o V}{2}\sum_{k=1}^{\infty} (-i)^k A_3(k)\delta(f_n + f_o - kf) \\ &+ \frac{I_o V}{2}\sum_{k=1}^{\infty} (-i)^k A_4(k)\delta(f_n + f_o + kf) \end{aligned} \quad (11)$$

where $\delta(f)$ is the Dirac delta function.

It is shown in Eq. (10) there are harmonic frequency peaks in the positions of $f = \pm f_0$, $f_0 \pm kf$, $-f_0 \pm kf$. For the positive half of the spectrum, the absolute value of amplitude $|A_n(k)|$ lowers following the Bessel function $J_0(r)$ and the sinc function sinc($f_0 \pm kf$) with increase of k, in both sides of the foundational frequency. Under conditions of f_s=100Hz, f_0=20Hz, f_v=2Hz, and r=0.85λ, spectrum of a temporal intensity array has been demonstrated in Fig. 2.

Based on Eq. (9) and Fig. 2, the best relative sampling frequency is supposed to minimize the possibility of spectrum overlap at both sides of half part of the spectrum. Therefore, the best relative sampling frequency is 4 because of the symmetric distribution of spectrum of Eq. (10). When the sampling frequency is higher than 4 times of phase-shifting frequency, it is theoretically all right, but the higher sampling frequency will greatly enhance the cost of the system.

A simulation with different relative sampling frequencies has been shown in Fig. 6. The smallest PV value is obtained when the sampling frequency is 100 Hz, when the relative sampling frequency is 4, which perfectly verifies the conclusion of Eq. (10). In a real testing process, it is not easy to fix a sampling frequency of exactly 4 times of phase-shifting rate. In that case, a sampling frequency between 3.5 to 4.5 times of phase-shifting frequency is much better than the lower and higher ones.

The best relative sampling frequency in previous spatial-time domain method is 50, which extremely restrains its phase-shifting frequency under a fixed sampling frequency. The statistic operation toward the distorted phase series in the spatial-time domain method and the TFD method are theoretically the same. With a fixed CCD sampling frequency, the anti-vibration ability of TFD method under a relative frequency of 50 has the same anti-vibration ability with the TSD method under the same condition. Therefore, the anti-vibration with a relative frequency of 50 is obviously much lower than that under the best relative frequency. This is why the capacity of anti-vibration ability of TFD method is much higher that of the time-spatial method.

5. Conclusions

In TFD phase-shifting interferometry, a series of distorted phase is obtained through a broadband filtering toward spectrum of intensity series from a particular pixel. A calculating value of original phase is produced from the linear statistics of the distorted phase array. Through the linear statistics, random noises are averaged into zero, and nonrandom noises are astringed to a nonzero which is independent to pixel index. After a spatial unwrapping operation, the reconstructed phase distribution has the same shape with the original wave front, differing with a pistol shift. Several simulations shown the effects of different factors to measuring accuracy, and reflect the importance of relative sampling frequency. In order to maximize the anti-vibration ability, the best relative sampling frequency is determined through a simulation and a theoretical analysis in presence of a single vibration. The best relative sampling frequency essentially explains the advantages of TFD interferometry over the previous TSD random phase-shifting method.

ACKNOWLEDGEMENT

This work was supported by the National Natural Science Foundation of China (NSFC) 60578053.

REFERENCES

1. J. H. Bruning, D. R. Herriott, J. E. Gallagher, D. P. Rosenfeld, A. D. White, and D. J. Brangaccio, “Digital wavefront measuring interferometer for testing optical surfaces and lenses,” Appl. Opt., Vol.13, No.11, pp. 2693-2703, 1974.
2. Leslie L. Deck, “Suppressing vibration errors in phase-shifting interferometry,” Proc. of SPIE, Vol. 6704, No. 670402, pp. 1-7, 2007.
3. Leslie L. Deck, “Suppressing phase errors from vibration in phase-shifting interferometry,” Appl. Opt., Vol.48, No. 20, pp. 3948-3960, 2009.
4. R. Smythe and R. Moore, “Instantaneous phase measuring interferometry,” Opt. Eng., Vol. 23, No. 4, pp: 361-364, 1984.
5. J. E. Millerd, N. J. Brock, “Methods and apparatus for splitting, imaging and measuring wave fronts in interferometry,” U. S. Patent 6, 304, 330, 2001.
6. James E. Millerd, Neal J. Brock, John B. Hayes, Michael B. North-Morris, Matt Novak, and James C. Wyant, “Pixelated phase-mask dynamic interferometer,” Proc. SPIE, Vol.5531, pp. 304-314, 2004.
7. Katsuyuki Okada, Hironobu Sakuta, Teruju Ose, et al, “Separate measurements of surface shapes and refractive index inhomogeneity of an optical element using tunable-source phase shifting interferometry,” Appl. Opt., Vol. 29, No. 22, pp. 3280-3285, 1990.
8. Leslie L. Deck, “Fourier-transform phase-shifting interferometry,” Appl. Opt., Vol. 42, No. 13, pp. 2354-2365 , 2003.
9. Qun Hao, Qiudong Zhu, Yao Hu, “Random phase-shifting interferometry without accurately controlling or calibrating the phase shifts,” Opt. Lett., Vol. 34, No. 8, pp. 1288-1290, 2009.
10. Tang Lei, “Noiseproof wavefront testing method in time-and spatial-domain,” Doctoral Dissertation for Doctor Degree of Beijing Institute of Technology, pp. 57-63, 2008.